Three-dimensional Finite Element Model of Three-phase Contact Line Dynamics and Dynamic Contact Angle

KONSTANTIN A. CHEKHONIN, VICTOR D. VLASENKO
Computing Center of the Far Eastern Branch of the RAS,
65 Kim Yu Chena, Khabarovsk 680000,
RUSSIAN FEDERATION

Abstract: - An unconventional model of three-phase contact liny dynamics is suggested for the numerical solution of the boundary value problem of dipping and spreading. The numerical modeling is conducted with the use of the finite-element method in Lagrange variables. The mathematical model of the process is described by the equation of motion, continuity, and natural boundary conditions on the free surface. To exclude the ity of viscous stresses in the mathematical model on three-phase contact lines (TPCL) there was suggested a gridded model of gliding that takes into consideration peculiarities of dissipative processes in the neighborhood of TPCL at the microlevel. To reduce oscillations of pressure in the neighborhood of TPCL, a finite element is used. The suggested method allows for natural monitoring of free surface and TPCL with an unconventional model for dynamic contact micro-angle. A stable convergent algorithm is suggested that is not dependent on the grid step size and that is tested through the example of a three-dimensional semispherical drop and a drop in the form of a cube. The investigations obtained are compared to well-known experimental and analytical results demonstrating a high efficiency of the suggested model of TPCL dynamics at small values of capillary number.

Key-Words: - Navier–Stokes equations, continuity equation, free surface, drop, gliding, adhesion, dynamic boundary angle, three-phase contact line, finite element method.

Received: January 14, 2023. Revised: November 8, 2023. Accepted: December 6, 2023. Published: January 23, 2024.

1 Introduction

The processes of dripping and spreading of a drop of liquid on solid and liquid surfaces are the initial and most important stages of many physicochemical phenomena accompanying modern technologies. For example, the building of microelectronic components, modeling of deformable biological membranes, the process of forming powder coatings, technology of settling micro-drops of ink in the conditions of ink-jet printing.

In the processes of dripping and spreading, there are hydrodynamical peculiarities: the presence of interphase or free surface and three-phase contact line (TPCL) that moves along a solid surface in a tangent direction for instance, a solid body-liquid-gas. The position of the interphase surface and TPCL in the given area is unknown in advance and is a part of the solution to a problem. The analytical solution of such boundary problems can seldom be obtained and the capabilities of an experimental investigation are very limited. Therefore, one of the basic tools of investigation of such type boundary problems is their numerical solution. Herewith, in the case of using mathematical model approaches the main difficulties are related to obtaining a solution in the TPCL area and building an effective computational algorithm.

Beginning from the 60-ties of the XX century, there has been completed a huge number of theoretical and experimental investigations at the presence of interphase boundary and TPCL. The overview of such works is described in the works, [1], [2]. However, despite much attention to the problem and numerous practical applications of the solution thereof, so far there has been no full understanding of the mechanisms of interaction of phase on the line of contact and related-to-them formation of the interface front, peculiarities of the contact line dynamics and liquid flow in its neighborhood in the conditions of dripping and spreading. The universal dependence between outer volume flow and local dynamics in the neighborhood of TPCL is absent, [3], [4].

When modeling static problems of the hydrodynamics of dripping, TPCL stays unmovable with a given static contact angle to a smooth surface determined under Young-Dupré law, [1], [3]. In dynamic problems, TPCL moves with a time-variant rate and dynamic contact angle. The problem of determining dynamic boundary angle (DBA) is multiscale. In basic DBA models, the microscopic

angle is supposed to be determined by intermolecular forces of short-range and to preserve its equilibrium value. The Microscopic DBA equal to the visually observed in experiments is determined by the kinematics of flow, TPCL moving rate, and properties of adhesion of liquid on a solid surface. All theoretical models contain unknown parameters, which need agreeing with the experiment and which hide the physics of dynamic processes in the neighborhood of TPCL. All empirical models are only applicable to certain conditions of flow and a limited circle of liquids and surfaces. In numerical modeling, the algorithm of implementing the selected model of DBA on the grid area is also all-important. In the works, [1], [2], [5], [6], [7], [8] it is noted that for obtaining approximated convergence it is necessary to use a grid dependence of the length of gliding with the use of advanced approximation of initial functions in the neighborhood of TPCL, which in its place requires the use of special "approaches" of their implementation. To a great degree, this impacts the kinematics of flow near TPCL, and as a consequence, the efficacy of modeling in comparison with the experiment, stability, and convergence of the numerical algorithm, [9], [10], [11], [12], [13], [14] [15], [16], [17], [18], [19], [20], [21].

The main requirements when building numerical models of the TPCL dynamics in the conditions of dripping and spreading are as follows: it is necessary to establish a monotonous dependence of microscopic and macroscopic dynamical contact angles ensuring the kinematics of movements of micro volumes in the neighborhood of TPCL in form of swell; determining the length of gliding from the rate of TPCL and volumetric parameters of flow, for instance, of the Reynolds or the Bond number; the rate of TPCL is a priori unknown and is a solution to the problem in implementing kinematic conditions. Therefore, additional assessments of its determination are needed that exclude its non-physic movements.

This work introduces a modeling of the flow of viscous incompressible liquid with a free surface of various conditions of dripping on solid walls with a strong effect of surface tension in comparison with gravitation and viscous forces. For the modeling, the method of finite elements in Lagrange variables, [22], [23] is applied. When applying the Laplace–Beltrami operator in transforming boundary conditions for the pressure jump on the free surface, [24], the order of derivatives on the free surface was reduced. This allowed for naturally including the boundary conditions of gliding on TPCL, its rate, and DBA. All the dynamic parameters of DBA flow are computed naturally in the nodes belonging to TPCL and do not require additional interpolation.

The use of setting up the problem in Lagrange variables allows for direct monitoring of free surface and TPCL, for excluding the nonlinearity of convective member and implementing a completely unexpressed algorithm of computation of the position of free surface with the DBA model built on equipoising Young's dynamic forces by viscous friction on TPCL with due consideration of the effect of the dynamical microscopic contact angle. All these are obtained in the frame of molecular-kinetic theory, [25] and agree with molecular-dynamic computation, [26], [27]. The algorithm is tested on the example of the spreading of viscous incompressible drop under the impact of surface tensions and gravitation forces in static and dynamic conditions of dripping and spreading on a smooth solid surface.

2 Building the Model of TPCL Movement

We shall consider the model of the movement of TPCL on the example of a problem of a drop spreading on a solid smooth base layer. Figure 1 introduces a computational area and details of the geometry of the area with contact angle θ.

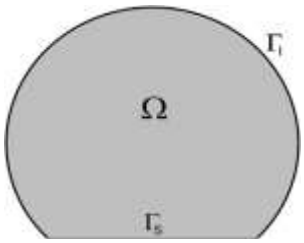

a)

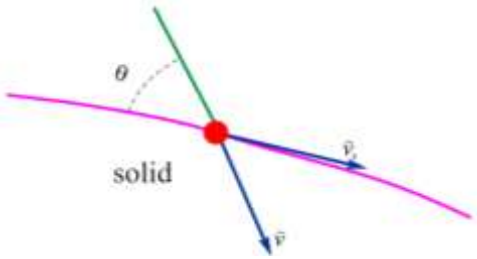

b)

Fig. 1: a) Viscous drop with free surface Γ_1 lying on solid base layer Γ_S, b) TPCL (red dot), revealed as the circular curve of intersection of boundaries Γ_1 and Γ_S

The balance of forces affecting TPCL can be presented as follows:

$$\boldsymbol{\sigma}\cdot\mathbf{n}+\beta\mathbf{u}+\gamma\left(\cos\theta-\cos\theta_S\right)\tilde{\mathbf{v}}_S\delta_{\partial\Gamma}, \qquad (1)$$

where, $\mathbf{u}$ – velocity vector, $\boldsymbol{\sigma}=-p\mathbf{I}+2\mu D\mathbf{u}$ – stress tensor, p – pressure, μ – dynamic coefficient of viscosity, $\mathbf{n}$ – vector of normal to free boundary Γ_1, $\mathbf{I}$ – unit tensor, γ – coefficient of surface tension at the inter-phase surface of liquid-air, $\delta_{\partial\Gamma}$ – Dirac delta function, $\tilde{\mathbf{v}}_S$ – singular vector of the tangent to solid wall, $\tilde{\mathbf{v}}$ – singular vector of the tangent to free surface.

If dynamic and static angles equal $\theta = \theta_S$, then the tilting angle of the free surface on TPCL to the solid wall in the process of spreading is constant and equals the static contact angle.

The majority of investigations when modeling exclude the consideration of dissipative processes at the microlevel in the neighborhood of TPCL, and only consider meso- and macro-levels applying the condition of static contact angle at meso-level (fir. 1), for instance, work, [28]. It's justified, since from the point of mechanics of continuum, the microregion is an area of the unavailability of the solution. However, the investigations, [29], show that the establishment of boundary conditions for dynamic contact angle at the microlevel as a static is incorrect. Moreover, the conducted molecular-dynamical calculations also show various mechanisms flowing in dissipative processes in the neighborhood of TPCL on various scales.

The idea of building the TPCL dynamics model consists of presenting the balance of forces on TPCL (1) at the microlevel or, in other words, building of correct boundary conditions for the TPCL macro-model. In such cases, the contact angles on TPCL are presented as microscopic. According to molecular-dynamical calculations, we shall express the coefficient of gliding in the form of a sum of Navier friction-gliding and the coefficient of friction on TPCL itself:

$$\beta=\beta_N+\beta_{CL}\delta_{\partial\Gamma}.$$

The coefficient of Navier friction-gliding distributes in the neighborhood of TPCL on the solid wall under exponential law from some given β_N with nearing of the gliding length $l_S=\mu/\beta_N$ to zero with distancing from it, i.e. no-slip condition.

We shall compute the coefficient of friction directly on TPCL from the relations molecular kinetic theory, [25]

$$\beta_{CL}=\frac{\kappa_B T}{K_0\lambda^3},$$

where, κ_B – Boltzmann constant, T – Kelvin temperature, K_0, λ – frequency and length of jumps of molecules of liquid.

A special difficulty in modeling the dynamics of TPCL appears in the case of hysteresis of contact angle, [1], [2]. In this care, there differ the advancing and the receding contact angles, which are not equal. Their difference is the one that forms the hysteresis. The difficulty is in the fact that TPCL is immovable for all angles located in the interval of the hysteresis and begins moving only at the angle leaving the interval of hysteresis. In this case, similar to the Signorini contact problems with friction, we get to the variational setting in the form of variational inequalities. To solve this problem, we shall apply Lagrange multipliers.

On the basis of the mathematical model of the considered problem we shall put Navier-Stokes equations and equation of continuity, [24]:

$$\rho\left[\frac{\partial\mathbf{u}}{\partial\mathbf{t}}+\mathbf{u}\cdot\nabla\mathbf{u}\right]=\nabla\cdot\boldsymbol{\sigma}+\rho g,\quad \nabla\cdot\mathbf{u}=0, \qquad (2)$$

where, ρ – density, g – gravitational acceleration.

We shall compute the system of equations (2) with the use of the following boundary conditions:

– on the free surface moving with kinematic condition:

$$\left(\frac{\mathrm{d}\mathbf{x}}{\mathrm{dt}}-\mathbf{u}\right)\cdot\mathbf{n}=0$$

we shall set up boundary dynamic boundary conditions consisting in the absence of tangent stresses and equality of normal to the sum of external and capillary pressures:

$$\mathbf{n}\cdot\boldsymbol{\sigma}\cdot\left(\mathbf{I}-\mathbf{nn}\right)=0,$$

$$-\mathbf{n}\cdot\boldsymbol{\sigma}-\mathbf{n}p_a=\frac{1}{\mathrm{Ca}}\kappa\mathbf{n},$$

where, $\mathbf{n}$ – vector of normal to free surface, κ – curvature of the free surface, Ca – capillary number, p_a – pressure over the free surface, which we accept as equal to zero without losing the solidarity of purpose.

At the lines of three-phase contact, we shall establish boundary conditions of gliding and impermeability, [23]

$$\mathbf{n_s}\cdot\left|\boldsymbol{\sigma}\right|\cdot\left(\mathbf{I}-\mathbf{n_s}\mathbf{n_s}\right)=\beta\mathbf{u}\cdot\left(\mathbf{I}-\mathbf{n_s}\mathbf{n_s}\right),\quad \mathbf{n_s}\cdot\mathbf{u}=0,$$

where, β – nondimensional parameter of gliding ($\beta = 0$ – complete gliding, $\beta = \infty$ – adhesion), $\mathbf{n_s}$ –

singular vector of normal to a solid wall in the neighborhood of TPCL.

Projection-fine-difference equations are reported in, [24], so we shall report here the peculiarities of numerical implementation with consideration of the hysteresis of the angle.

With due consideration of the angle hysteresis, the smallness of the Reynolds number and the condition (1) in the neighborhood of TPCL, the projection-fine-difference equations of the problem can be expressed as follows:

To find $(\mathbf{u}_h^{n+1}, p_h^{n+1}) \in W_h \times Q_h$ consistent with the equation:

$$\int_\Omega 2\mu D\mathbf{u}_h^{n+1} : D\mathbf{w}_h \mathrm{d}\Omega - \int_\Omega p_h^{n+1} \nabla \cdot \mathbf{w}_h \mathrm{d}\Omega =$$

$$= \int_{\Gamma_h^{n+1}} \gamma \mathbf{P}^{n+1} : \nabla \mathbf{w}_h \mathrm{d}\Gamma - \int_{\partial\Gamma_h^{n+1}} (\gamma \mathbf{M} + \lambda_h^{n+1}) \tilde{\nu}_S \cdot \mathbf{w}_h \mathrm{d}\partial\Gamma -$$

$$- \int_{\partial\Omega} \beta \mathbf{u}_h^{n+1} \cdot w_h \mathrm{d}\Omega, \qquad (3)$$

$$\int_\Omega q_h \nabla \cdot \mathbf{u}_h^{n+1} \mathrm{d}\Omega + \int_\Omega \tau_h \nabla p_h^{n+1} \cdot \nabla q_h \mathrm{d}\Omega = 0, \qquad (4)$$

$$\int_{\partial\Gamma_h^{n+1}} \eta_h [\cos\theta - \cos\theta_S (\mathbf{u}_h \cdot \tilde{\mathbf{v}}_S)] \mathrm{dS} = 0, \qquad (5)$$

where, $M = \frac{\gamma_{S+} - \gamma_{S-}}{\gamma}$, $\theta_S = \arccos \mathrm{M}$, i.e. $\gamma \cos\theta_S = \gamma_{S+} - \gamma_{S-}$ – Young-Dupré law, $\mathbf{P} = \mathbf{I} - \mathbf{n} \otimes \mathbf{n}$ ($P_{ij} = \delta_{ij} - n_i n_j$), $\tilde{\tau}_h = \tilde{c} \frac{h}{\|\mathbf{u}_h\|}$ – parameter of the equation stability, λ_h, η_h – Lagrange multipliers, $\tilde{c}$ =0.5.

3 Results of Computations

We shall consider the spreading of the viscous drop (Figure 1) with known initial θ_0 and static contact angles θ_S under the effect of the surface tension forces. Density, viscosity, and surface tension coefficient shall be taken to be equal to one. We believe that the gravitation forces are sufficiently small (the Bond number << 1). At the initial moment, the liquid is moveless and occupies the volume equal to V, which doesn't change in the process of spreading. We shall take Navier–Stokes equations and equations of continuity as a basis of mathematical description. For the $\boldsymbol{\sigma} \cdot \mathbf{n} \cdot \mathbf{w} dV$ member for normal stresses, we shall substitute the right part of the equation (3) with the additional condition (5). The introduction of Lagrange multipliers is needed in the case of contact angle hysteresis since they ease out the conditions in the form of inequation at the ratio of the contact angle and the rate of TPCL. We shall obtain the projection-fine-difference equations in Lagrange variables by way of adding to the left part of the equation (3) a nonstationary member of Navier–Stokes equations or consider the solution (3)-(5) as a sequence of quasistatic problems with integrating of kinematic conditions on $\mathbf{\Gamma_1}$ free surface by the implicit scheme.

We shall investigate the grid convergence of the suggested algorithm based on the spreading of the drop in the form of a semisphere with an initial angle of 90 degrees and a static angle of 60 degrees. The initial radius of the drop equals 0,5. For the case, when the capillary number is substantially smaller than one, the radius of spreading of the drop in the function from the visual contact angle can be expressed as follows

$$R_d^3 = \left(\frac{3V_0}{\pi}\right) \Phi(\theta_d),$$

$$\Phi(\theta_d) = \frac{\sin^3 \theta_d}{2 - 3\cos\theta_d + \cos^3 \theta_d}. \qquad (6)$$

After differentiating equation (6) by time, we obtain a regular differential equation of evolution of the radius of spreading in the function from the rate of the rate of contact angle changing, which is solved by the Runge–Kutta method. The spreading radius of the drop to the static state can be calculated from the relation (6) by substituting the static contact angle with the condition of the volume stationarity. In our case, for the static angle of 60 degrees, the relation of the static spreading radius to the initial equals 1,276186.

We shall produce the numerical solution of the problem (3)-(5) on the sequence of grids.

Figure 2 shows the grid convergence of the suggested algorithm and the comparison of the evolution of the spreading radius in the functions from the time with an analytic solution at values of the microscopic parameters of friction on TPCL β_N = 100, β_{CL} = 1. From the calculation results there follows a grid convergence of the considered algorithm and a good correspondence of the evolution of the spreading radius to the analytic solution.

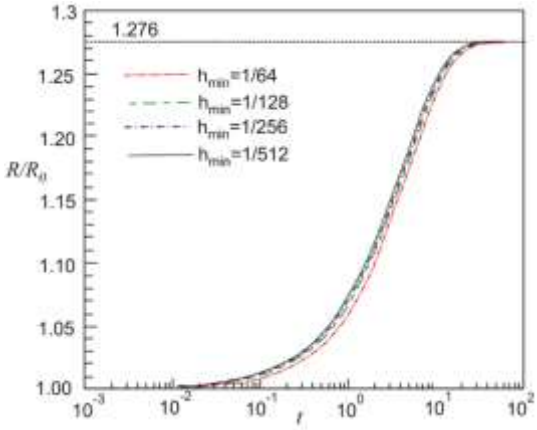

Fig. 2: Evolution of spreading radius of semispherical drop in time t to a static contact angle of 60 degrees

Figure 3 shows the influence of the changing of dynamical parameters of friction of TPCL on the evolution of the radius of spread. The computational experiment was conducted on the grid with minimal step on TPCL equal to h_{min} = 1/64. It follows from the calculation results that the growth coefficient of Navier friction-gliding has a weak effect on the evolution of the radius of spreading, but has a strong effect on the grid convergence. The growth of the friction coefficient β_{CL} substantially slows down the evolution of the radius of spreading and reduces the effective length of gliding L_S (Figure 3).

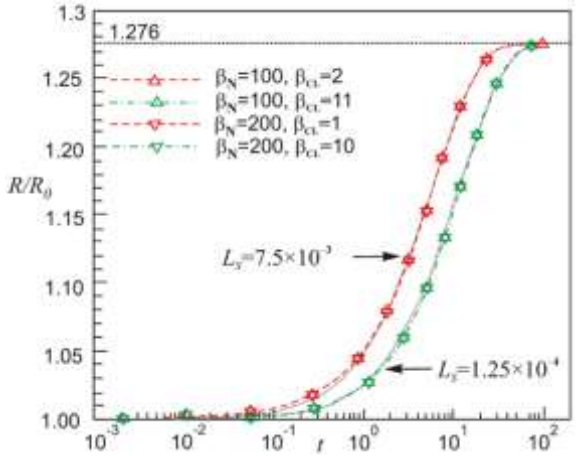

Fig. 3: Influence of changing in parameters of friction on TPCL on the evolution of radius of spreading

Now, therefore, the contribution of friction coefficients on TPCL in the efficiency of the considered algorithm becomes clear.

Now, we shall conduct a comparison of the calculation results with the experiment of drop spreading conducted in work, [30]. For the calculations, there was taken the value of static contact angle θ_S = 54°. The initial radius of the drop was taken as equal to 0,5 with the center of mass (0; 0.48) on a solid base layer. The liquid viscosity was normalized and was taken as equal to 1. The calculation results are stated in Figure 4.

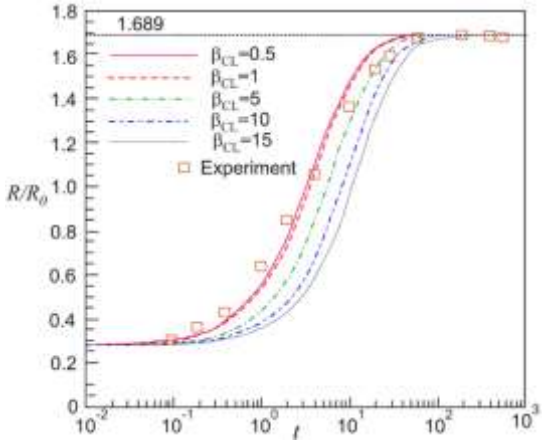

Fig. 4: Evolution of radius of spreading of a drop in time t at various values of friction coefficient with h_{min} = 0.01, □ – experimental result, [30]

It follows from the calculation results that the coefficient of friction on TPCL is an adjustable parameter of the model of the TPCL dynamics (for the correspondence of the numerical model to the experiment). In our case, the best result is obtained at friction coefficient β_{CL} = 0.5. In addition, the calculation analysis shows that the suggested model of the TPCL dynamics does not correspond to the initial period of spreading of the drop, which is inertial. The model requires clarification by way of dependence of the friction coefficient on TPCL from the TPCL rate. It must be noted, that all the above-stated investigations were conducted in a three-dimensional set-up. Figure 5 illustrates an expressed three-dimensional case of the spreading of the drop of the initial form of a cube, initial contact angle of 90 degrees and a static contact angle of 60 degrees. The calculation results show a satisfactory agreement with the drop form of a constant volume in a static state. In all the calculations, the drop volume loss didn't exceed 0.01% at the static contact angle detection error, not above 0,1 degree.

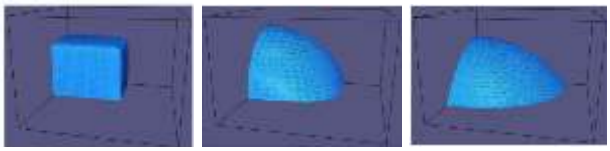

t = 0.0 s t = 0.5 s t = 1.0 s

Fig. 5: Spreading of a drop in the form of a cube lying on the solid base layer

The peculiarities of modeling a drop flow with a hysteresis of the angle of dripping are considered in the example of a drop lying on the oblique surface (Figure 6).

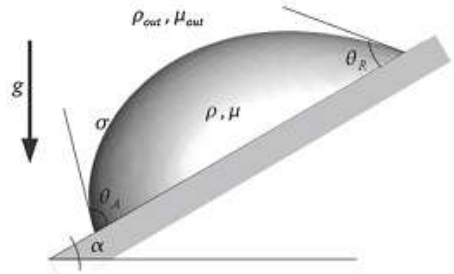

Fig. 6: Determining parameters of drop on the oblique surface

All these methods consist in the observance of the following conditions for normal rate U_{cl} of contact line:

$$U_{cl} < 0 \text{ if } \theta_d < \theta_R,$$
$$U_{cl} = 0 \text{ if } \theta_R \le \theta_d \le \theta_A,$$
$$U_{cl} > 0 \text{ if } \theta_A < \theta_R.$$

The oblique angle of surface α_c in the beginning of the movement can be obtained by watching the balance of forces affecting the drop: $\sin\alpha_c = \frac{\kappa}{a}\frac{3}{4\pi}(\cos\theta_R - \cos\theta_A)Eo^{-1}$, where, $Eo = \rho g a^2/\sigma$ – the Eötvös number, a – drop diameter, so the critical contact angle changes as $(\cos\theta_R - \cos\theta_A)Eo^{-1}$ and depends on the form of the contact line. Figure 7 shows the evolution of the linear rate of three-phased contact in the dependence on the hysteresis of the angle of dripping, where $Ca \approx \frac{4}{3C}Eo(\sin\alpha - \sin\alpha_c)$.

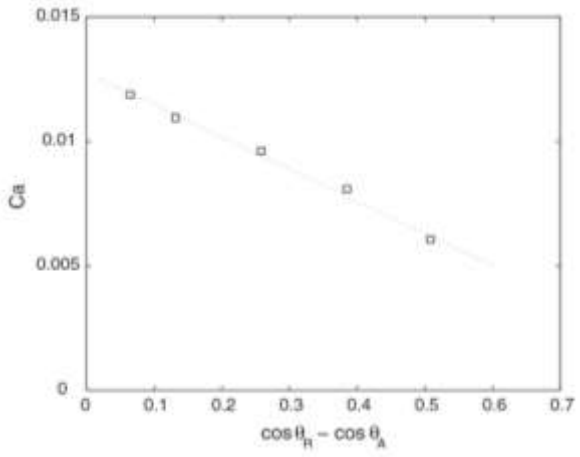

Fig. 7: Effect of hysteresis on velocity of liquid fall at α=50°

Ca is illustrated as a function $\cos\theta_R - \cos\theta_A$,
□ – modeling, ····· – y = 0,0128 - 0,013x

4 Conclusion

As the investigation results there was suggested a correct dynamic model of TPCL and a variational formulation of a problem with variable dynamic contact micro-angle. To exclude the singularity of tangent stresses on TPCL, the coefficient of Navier friction-gliding is applied. The friction coefficient on TPCL is adjustable for the comparison with an analytical solution or experiment. There was suggested a stable, not-depending on a grid state, convergent numerical algorithm that is tested on the example of a three-dimensional semispherical drop and a drop in the form of a cube. The investigations obtained are compared with the known experimental and analytical results demonstrating a high efficiency of the suggested model of the TPCL dynamics at small values of capillary number. These investigations may be useful for solving and forecasting such situations as, for instance, the production of ink for ink-jet printing, applying of liquid coatings and drainage in porous media, spreading of pesticides on leaves, whole blood dripping, spreading and drying of a blood serum drop.

References:

[1] Bonn D., Eggers J., Indekeu J., and Meunier J. Wetting and spreading, *Reviews of Modern Physics*, Vol. 81, 2009, pp. 739-805.

[2] Wörner M., Numerical modeling of multiphase flows in microfluidics and micro process engineering: a review of methods and applications, *Microfluidics and nanofluidics*, Vol. 12(6), 2012, pp. 841-886.

[3] Shikhmurzaev Y.D. Solidification and dynamic wetting: a unified modeling framework, *Physics of Fluids*, Vol. 33, 2021, pp. 072101.

[4] Shikhmurzaev Y.D. Some dry facts about dynamic wetting, *The European Physical Journal. Special Topics*, Vol. 197(1), 2011, pp. 47-60.

[5] Snoeijer J.H., and Andreotti B. Moving contact lines: scales, regimes, and dynamical transitions, *Annual Review of Fluid Mechanics*, Vol. 45, 2013, pp. 269-292.

[6] Shikhmurzaev Y.D. Moving contact lines and dynamic contact angles: a 'litmus test' for mathematical models, accomplishments and

new challenges, *The European Physical Journal. Special Topics*, Vol. 229, Issue 10, 2020, pp. 1979-1987.

[7] Kirkinis E., and Davis S.H. Hydrodynamic Theory of Liquid Slippage on a Solid Substrate Near a Moving Contact Line, *Physical Review Letters*, Vol. 110, 2013, 234503.

[8] Della Rocca, G.V. *A Novel Methodology for Simulating Contact-Line Behavior in Capillary-Driven Flows*. California Institute of Technology, 2014.

[9] Lācis U., Johansson P., Fullana T., Hess B., Amberg G., Bagheri S., and Zaleski S. Steady moving contact line of water over a no-slip substrate. Challenges in benchmarking phase-field and volume-of-fluid methods against molecular dynamics simulations, *The European Physical Journal Special Topics*, Vol. 229, 2020, pp. 1897–1921.

[10] Shin S., Chergui J., and Juric D. Direct simulation of multiphase flows with modeling of dynamic interface contact angle, *Theoretical and Computational Fluid Dynamics*, Vol. 32, 2018, pp. 655–687.

[11] Lea N.T., Coquerelleb M., and Glocknerb S. Numerical simulation of moving contact line in wetting phenomena using the Generalized Navier Boundary Condition, 24 Congrès Français de Mécanique. Brest, 26 au 30 Août 2019. https://cfm2019.sciencesconf.org/245813.html

[12] Fakhari A., and Bolster D. Diffuse interface modeling of three-phase contact line dynamics on curved boundaries: A lattice Boltzmann model for large density and viscosity ratios, *Journal of Computational Physics*, Vol. 334, 2017, pp. 620–638.

[13] Esteban A., Gómez P., Zanzi C., López J., Bussmann M., and Hernández J. A contact line force model for the simulation of drop impacts on solid surfaces using volume of fluid methods, *Computers & Fluids*, Vol. 263, 2023, 105946.

[14] Brutin D., and Starov V. Recent advances in droplet wetting and evaporation, *Chemical Society Reviews*, Vol. 47, 2018, pp. 558-585.

[15] Zaytoon M.S., and Hamdan M.H. Parallel Flow of a Pressure-Dependent Viscosity Fluid through Composite Porous Layers, *WSEAS Transactions on Fluid Mechanics*, Vol. 17, 2022, pp. 1–9, https://doi.org/10.37394/232013.2022.17.1.

[16] Radhika T.S.L., and Rani T.R. On a Study of Flow Past Non-Newtonian Fluid Bubbles, *WSEAS Transactions on Fluid Mechanics*, Vol. 16, 2021, pp. 79–91, https://doi.org/10.37394/232013.2021.16.8.

[17] Makanda G., and Shaw S. Numerical Analysis of the Bivariate Local Linearization Method (BLLM) for Partial Differential Equations in Casson Fluid Flow, *WSEAS Transactions on Fluid Mechanics*, Vol. 14, 2019, pp. 131–141.

[18] Shahmardi A., Rosti M.E., Tammisola O., and Brandt L. A fully Eulerian hybrid immersed boundary-phase field model for contact line dynamics on complex geometries, *Journal of Computational Physics*, Vol. 443, 2021, 0468.

[19] Guo Z., Rachid Hakkou R., Yang J., and Wang Y. Effects of surface heterogeneities on wetting and contact line dynamics as observed with the captive bubble technique, *Colloids and Surfaces A: Physicochemical and Engineering Aspects*, Vol. 615, 2021, 126041.

[20] Sourais A.G., Markodimitrakis I.E., Chamakos N.T., and Papathanasiou A.G. Droplet evaporation dynamics on heterogeneous surfaces: Numerical modeling of the stick-slip motion, *International Journal of Heat and Mass Transfer*, Vol. 207, 2023, 123992.

[21] Esteban A., Gómez P., Zanzi C., López J., Bussmann M., and Hernández J. A contact line force model for the simulation of drop impacts on solid surfaces using volume of fluid methods, *Computers & Fluids*. Vol. 263, 2023, 105946.

[22] Bulgakov V.K., and Chekhonin K.A. Fundamentals of the theory of mixed finite element method, Khabarovsk: Publishing house Khabarovsk: Polytechnic. Institute, 1999 (In Russian).

[23] Chekhonin K.A., and Sukhinin P.A. Numerical modeling of filling the axially symmetric channel with non-linearly viscoelastic fluid taking into account π effect, *Inzhenerno-fizicheskii zhurnal*, Vol. 72(5), 1999, pp. 881–886 (In Russian).

[24] Chekhonin K.A., and Vlasenko V.D. Modelling of capillary coaxial gap filling with viscous liquid, *Computational Continuum Mechanics*, Vol. 12, 2019, pp. 313–324 (In Russian).

[25] Blake T.D. The physics of moving wetting lines, *Journal of Colloid and Interface Science*, Vol. 99, 2006, pp. 1–13.

[26] Ren W., and Weinan E. Derivation of continuum models for the moving contact line problem based on thermodynamic principles,

Communications in Mathematical Sciences, Vol. 9, 2011, pp. 597–606.

[27] Qian X. P., Wang X-P., and Sheng P., A variational approach to moving contact line hydrodynamics, *Journal of Fluid Mechanics*, Vol. 564, 2006, pp. 333–360.

[28] Voinov O.V. Hydrodynamics of wetting, *Fluid Dynamics*, Vol. 11, 1976, pp. 714–721.

[29] Sui Y., Ding H., and Spelt P.D.M. Numerical Simulations of Flows with Moving Contact Lines, *Annual Review of Fluid Mechanics*, Vol. 46, 2014, pp. 97–119.

[30] Zosel A. Studies of the wetting kinetics of liquid drops on solid surfaces, *Colloid and Polymer Science*, Vol. 271, 1993, pp. 680–687.

Contribution of Individual Authors to the Creation of a Scientific Article (Ghostwriting Policy)

The authors equally contributed to the present research, at all stages from the formulation of the problem to the final findings and solution.

Sources of Funding for Research Presented in a Scientific Article or Scientific Article Itself

No funding was received for conducting this study.

Conflict of Interest

The authors have no conflicts of interest to declare that are relevant to the content of this article.